Intrapulse depolarization in optical fibers: a classical analog of spin decoherence

Q. Lin and Govind P. Agrawal

Institute of Optics, University of Rochester, Rochester, New York 14627

Received September 22, 2004

We show that the combination of cross-phase modulation and polarization-mode dispersion inside optical fibers leads to a novel phenomenon of intrapulse depolarization manifested as different random states of polarization across the pulse profile. Such polarization evolution of optical pulses is directly analogous to the phenomenon of spin decoherence in semiconductors or pseudospin relaxation in atoms. © 2005 Optical Society of America

OCIS codes: 060.4370, 190.4370, 060.5060, 260.5430.

Some physical systems, although quite different in their origins, can exhibit the same dynamic behavior. A well-known example is the similarity between the spin precession of an electron in a magnetic field[1–4] and the interaction of a two-level atom with an optical field.[5,6] An electron in a superposition state of Zeeman sublevels precesses its spin at a Larmor frequency until environmental factors induce decoherence.[1–4] In the case of a two-level atom (modeled as a pseudospin) an optical field induces Rabi oscillations of the atomic dipole, while vacuum or laser fluctuations or atomic collisions relax the pseudospin motion.[5,6] Spin and pseudospin decoherence is considered to be a universal phenomenon associated with two-level quantum systems. Here we show that it has a classical analog in the polarization evolution of an optical pulse propagating inside a fiber in the presence of both polarization-mode dispersion (PMD) and cross-phase modulation (XPM). The combined effect of these two mechanisms leads to a novel phenomenon of intrapulse depolarization in a fashion analogous to spin decoherence in quantum systems.

To illustrate the underlying physics as simply as possible, we consider a pump–probe configuration with two copropagating waves at frequencies ω_p and ω_s. The pump wave has a peak power much higher than the probe (called signal from now on), such that it modulates the phases of both waves through self-phase modulation and XPM, but those induced by the signal are assumed to be negligible. Considering the third-order instantaneous nonlinear response of silica glass, we obtain the following vector equations governing wave propagation inside an optical fiber[7]:

$$\frac{\partial|A_p\rangle}{\partial z}+\delta\frac{\partial|A_p\rangle}{\partial\tau}=-\frac{i\omega_p}{2}\mathbf{B}\cdot\boldsymbol{\sigma}|A_p\rangle+\frac{i\gamma}{3}[2\langle A_p|A_p\rangle+|A_p^*\rangle\langle A_p^*|]|A_p\rangle, \tag{1}$$

$$\frac{\partial|A_s\rangle}{\partial z}=-\frac{i\omega_s}{2}\mathbf{B}\cdot\boldsymbol{\sigma}|A_s\rangle+\frac{2i\gamma}{3}[\langle A_p|A_p\rangle+|A_p\rangle\langle A_p|+|A_p^*\rangle\langle A_p^*|]|A_s\rangle, \tag{2}$$

where $|A_p\rangle$ and $|A_s\rangle$ are the Jones vectors for the pump and the signal,[8] respectively, δ describes the group-velocity mismatch (GVM) between them; γ is the nonlinear parameter; and $\boldsymbol{\sigma}$ is the Pauli spin vector.[8] We ignored the group-velocity dispersion assuming that pulses are relatively wide and experience little broadening. We also neglected PMD-induced differential group delay within each wave because it is negligible for the fiber lengths considered here (a few kilometers).

Vector $\mathbf{B}$ represents random birefringence. It induces fast variations in the state of polarization (SOP) on a length scale related to birefringence correlation length l_c ($\sim$10 m),[9] typically much shorter than the length over which the nonlinear effects occur ($\sim$1 km for a modest peak power). As a result, rapid SOP variations average over the nonlinear effects and lead to a polarization-independent self-phase modulation.[7] After a rotating frame in which the pump SOP does not change is chosen, Eqs. (1) and (2) reduce to[7]

$$\frac{\partial|A_p\rangle}{\partial z}+\delta\frac{\partial|A_p\rangle}{\partial\tau}=i\gamma_e P|A_p\rangle, \tag{3}$$

$$\frac{\partial|A_s\rangle}{\partial z}=\frac{i\gamma_e}{2}P(3+\hat{p}\cdot\boldsymbol{\sigma})|A_s\rangle-\frac{i}{2}\Omega\mathbf{b}\cdot\boldsymbol{\sigma}|A_s\rangle, \tag{4}$$

where $\gamma_e=8\gamma/9$, $\Omega=\omega_s-\omega_p$, $P=\langle A_p|A_p\rangle$ is the pump power, and unit vector $\hat{p}=\langle A_p|\boldsymbol{\sigma}|A_p\rangle/P$ represents the pump SOP on the Poincaré sphere.[8]

Random birefringence enters through vector $\mathbf{b}(z)$, related to $\mathbf{B}(z)$ by a rotation in the Stokes space. Because fiber length and nonlinear length are both typically much longer than birefringence correlation length l_c, the situation we encounter here corresponds to the motional narrowing regime of spin relaxation.[1,3] As a result, we can model $\mathbf{b}$ as a three-dimensional Markovian process whose first- and second-order moments are given by $\overline{\mathbf{b}(z)}=0$ and $\overline{\mathbf{b}(z_1)\mathbf{b}(z_2)}=(D_p^2/3)\vec{I}\delta(z_2-z_1)$, where the overbar denotes an average over birefringence fluctuations, $\vec{I}$ is the third-order unit tensor, and $D_p=(l_c\overline{|\mathbf{b}|^2})^{1/2}$ is the PMD parameter of the fiber.

Equations (3) and (4) show that $P(z,\tau)=P(0,\tau-\delta z)$, but signal power profile $S(z,\tau)\equiv\langle A_s|A_s\rangle=S(0,\tau)$.

0146-9592/05/080821-3/$15.00

However, the signal SOP changes in a random fashion. To consider polarization effects for the signal, we convert Eq. (4) into Stokes space by introducing a unit Stokes vector as $\hat{s}=\langle A_s|\boldsymbol{\sigma}|A_s\rangle/S$. From Eq. (4), $\hat{s}(z,\tau)$ is found to satisfy

$$\partial\hat{s}/\partial z=(\Omega\mathbf{b}-\gamma_e P\hat{p})\times\hat{s}. \tag{5}$$

The pump pulse changes the signal SOP through XPM-induced nonlinear polarization rotation, whereas PMD perturbs it randomly at a rate dictated by the magnitude of $\Omega\mathbf{b}$.

Equation (5) is isomorphic to the Bloch equation governing the motion of spin density in a solid.[1–4] The pump acts like a static magnetic field, and perturbations induced by PMD correspond to a fluctuating magnetic field induced by nuclei or phonons. Clearly the signal polarization would evolve along the fiber statistically in a fashion similar to the phenomenon of spin decoherence in time. This can be seen clearly when Eq. (5) is averaged over random $\mathbf{b}$ to obtain[10] $\partial\bar{\hat{s}}/\partial z=-\eta\bar{\hat{s}}-\gamma_e P\hat{p}\times\bar{\hat{s}}$, where η is the polarization relaxation rate related to PMD diffusion length L_d as $\eta=1/L_d=(D_p\Omega)^2/3$. Statistically, PMD causes signal polarization to relax along the fiber. However, XPM forces signal polarization to precess around pump Stokes vector $\hat{p}$ with a Larmor frequency of $\gamma_e P$. The global SOP of the signal, $\hat{S}(z)\propto\int_{-\infty}^{+\infty}\langle A_s|\boldsymbol{\sigma}|A_s\rangle d\tau/\int_{-\infty}^{+\infty}\langle A_s|A_s\rangle d\tau$, would evolve analogous to macroscopic magnetization in semiconductors.

There is one crucial difference between quantum spin dynamics and classical pulse propagation. In a quantum system, spin flipping requires energy dissipation, resulting in different longitudinal and transversal relaxation times, and electrons relax eventually to a thermal equilibrium among the Zeeman sublevels.[1–3] However, no such levels exist in a classical system, and PMD-induced polarization relaxation is uniform in three dimensions of the Stokes space. The signal SOP is completely randomized on the Poincaré sphere after a sufficiently long distance. In the absence of a pump, PMD changes the signal SOP randomly but uniformly across the entire signal pulse, resulting in no intrapulse decoherence. Similarly, in the absence of PMD, a pump pulse induces inhomogeneous but coherent polarization precession across the signal pulse, again creating no intrapulse decoherence. However, the combination of XPM and PMD produces a new effect that we refer to as intrapulse depolarization (IPD).

IPD can be quantified by the relative orientation of the signal SOPs at two different times. Defining $\hat{s}_1=\hat{s}(z,\tau_1)$ and $\hat{s}_2=\hat{s}(z,\tau_2)$, we introduce a scalar averaged quantity $d=\hat{s}_1\cdot\hat{s}_2$ as the IPD coefficient. Note that $\hat{s}_1$ and $\hat{s}_2$ evolve according to Eq. (5) with different pump powers. Even though they are defined in a relative rotating frame, d is invariant to such a global polarization rotation. Averaging over the random birefringence,[10] we obtain the following equations governing the evolution of the IPD coefficient:

$$\partial d/\partial z=\gamma_e P_- U, \tag{6}$$

$$\partial U/\partial z=-\eta U+\gamma_e P_-(V-d), \tag{7}$$

$$\partial V/\partial z=-3\eta V+\eta d, \tag{8}$$

where $P_-=P(z,\tau_2)-P(z,\tau_1)$, and U and V were introduced as $U=\hat{p}\cdot(\hat{s}_1\times\hat{s}_2)$ and $V=\hat{p}\cdot(\hat{s}_1\hat{s}_2)\cdot\hat{p}$.

To show how $d(z,\tau_1,\tau_2)$ changes along the fiber, we consider first the case of a signal pulse much wider than the pump pulse and neglect GVM for simplicity ($\delta=0$, corresponding to choosing wavelengths of two waves symmetrically around the zero-dispersion wavelength λ_0). Time τ_1 is set outside the pump pulse (no XPM), but τ_2 is set at the peak of the pump pulse where XPM is maximum. Figure 1 shows d as a function of $\xi=z/L_n$ for three values of the ratio $\mu=L_n/L_d$, where the nonlinear length is defined as $L_n=(\gamma_e P_0)^{-1}$ and P_0 is the peak power of the pump pulse. The ratio μ plays an important role as it governs the relative length scales of the PMD and XPM processes. Numerical simulations based on Eqs. (1) and (2) are also presented in Fig. 1. Simulations were carried out for a 5-km-long fiber with $\gamma=2\ \mathrm{W^{-1}/km}$, $D_p=0.2\ \mathrm{ps/(km)^{1/2}}$, $l_c=10$ m, $\lambda_0=1550$ nm, and $\beta_3=0.1\ \mathrm{ps^3/km}$. For completeness, group-velocity dispersion, which as well as GVM can be obtained from β_3, was indeed included in the simulations. The fiber is divided into 10-m-long sections with birefringence varying randomly from section to section. The FWHM of the Gaussian pump pulse is 166.5 ps. Statistical averages are computed with 1000 realizations. The good agreement justifies the use of a simple model based on Eqs. (6)–(8).

If the pump and signal are copolarized at the input end (solid curves), a situation that corresponds to the Faraday geometry in the spin analogy,[3] little nonlinear precession of SOP occurs. When $L_d\gg L_n$ ($\mu\ll 1$), d decays slowly along the fiber as PMD effects occur over a length scale much longer than L_n. When the

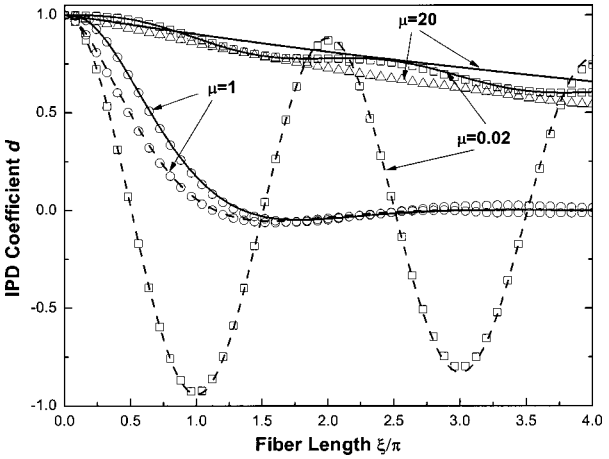

Fig. 1. IPD coefficient d for three values of $\mu=L_n/L_d$. Solid and dashed curves show the Faraday and Voigt geometries, respectively. Symbols show the simulation results performed with $P_0=1.41$ W. $\mu=0.02,1,20$ corresponding to $\Omega/2\pi=0.31$, 2.19, 9.77 THz, respectively.

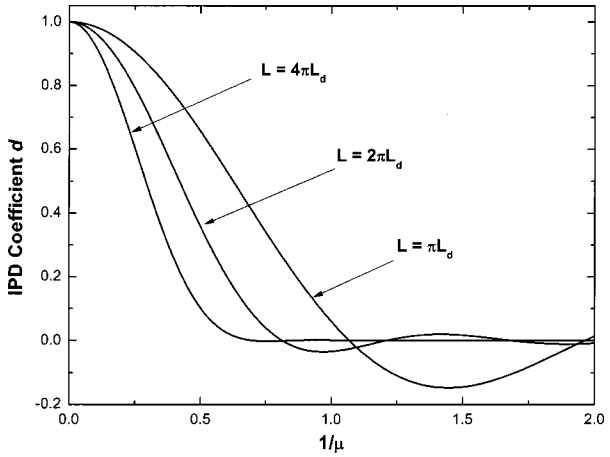

Fig. 2. IPD coefficient d as a function of $1/\mu=\gamma_e P_0 L_d$ for three fiber lengths in the Faraday geometry.

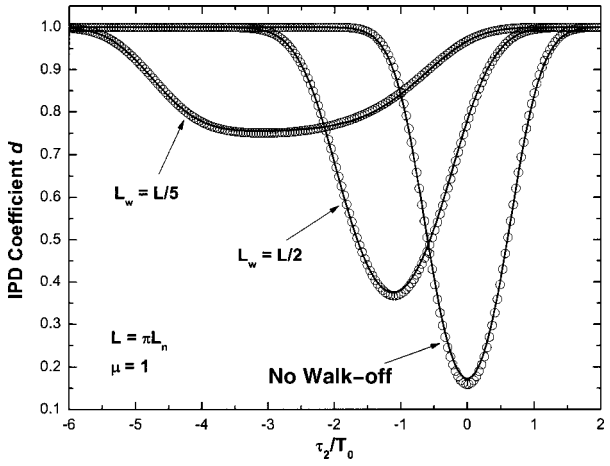

Fig. 3. IPD across the signal pulse for three walk-off lengths L_w. $L=\pi L_n$ and $\mu=1$. Simulation results (circles) use $\Omega/2\pi=1.09$ THz and $P_0=0.353$ W in the same fiber as Fig. 1. The width of the pump pulse is $T_0=\mathrm{FWHM}/1.665$.

two lengths become comparable ($\mu\approx 1$), XPM and PMD affect each other strongly, resulting in considerable IPD. As seen in Fig. 1, d decreases rapidly and becomes almost zero for $\xi>2$. However, when $L_d \ll L_n$ ($\mu\gg 1$), $\hat{s}$ changes randomly within a diffusion length even before XPM has any chance to act. Because of its averaging, the XPM effects become polarization independent, and the intrapulse polarization coherence is significantly recovered.

When $\hat{p}$ and $\hat{s}$ are initially orthogonal (corresponding to the Voigt geometry in spin precession[3]), the dashed curve for $\mu=0.02$ in Fig. 1 shows that d exhibits relaxation oscillations that are analogous to the free-induction decay in spin (pseudospin) relaxation dynamics.[1,5] These oscillations are suppressed by PMD, and maximum IPD occurs when $\mu\approx 1$. In contrast, when $\mu\gg 1$, not only are precessions suppressed, but IPD is also considerably reduced because PMD-induced rapid SOP variations average out the XPM-induced nonlinear polarization rotation.

IPD strongly depends on the pump power. Figure 2 shows d as a function of $1/\mu\equiv\gamma_e P_0 L_d$ for a fixed L_d in the Faraday geometry (a similar behavior occurs for the Voigt geometry). If the pump power is small, little IPD occurs even for $L\gg L_d$, although the global SOP of the signal varies randomly. IPD increases dramatically with pump power, and $d\to 0$ when $\mu^{-1}\approx 0.7$ for $L=4\pi L_d$. Spin decoherence induced by a magnetic field and its effects on photoluminescence (the Hanle effect) are widely used for measuring the spin relaxation time.[2,3] Analogously, the sensitivity of IPD to pump power might provide a simple means of PMD characterization.

Evolution of the signal polarization depends on the local interaction between PMD and XPM along the fiber. Interplay between PMD and XPM transfers spatial randomness of fiber birefringence into temporal randomness of signal polarization. Figure 3 shows IPD induced by a Gaussian pump pulse. In the temporal region outside the pump pulse, the signal only experiences PMD, and thus no IPD occurs. But within the overlap region, the signal SOP is affected by both PMD and XPM. If walk-off is zero, IPD is relatively large in the vicinity of the pump peak. Pulse walk-off broadens the depolarization region but reduces the IPD magnitude because of a decrease in the XPM strength.

In conclusion, we have shown that the combination of XPM and PMD leads to the novel phenomenon of intrapulse depolarization. We have also discussed how this behavior is analogous to spin and pseudospin decoherence in two-level quantum systems. From a practical perspective, such intrapulse depolarization affects the phase and chirp imposed on the signal pulse and leads to spectral distortion. It would affect the performance of XPM-based nonlinear fiber devices such as optical switches and wavelength converters. It would also affect PMD monitoring and PMD compensation in communication systems based on the measurement of degree of polarization.

The authors thank J. H. Eberly for helpful discussions. This work was supported by the National Science Foundation under grant ECS-0320816.

References

1. C. P. Slichter, *Principles of Magnetic Resonance*, 3rd ed. (Springer, New York, 1990).
2. F. Meier and B. Zakharchenya, eds., *Optical Orientation* (North-Holland, New York, 1984).
3. D. Awschalom, D. Loss, and N. Samarth, eds., *Semiconductor Spintronics and Quantum Computation* (Springer, New York, 2002).
4. Y. Semenov and K. Kim, Phys. Rev. Lett. **92**, 026601 (2004), and references therein.
5. L. Allen and J. H. Eberly, *Optical Resonance and Two-Level Atoms* (Wiley, New York, 1975).
6. J. H. Eberly, K. Wódkiewicz, and B. W. Shore, Phys. Rev. A **30**, 2381 (1984), and references therein.
7. Q. Lin and G. P. Agrawal, J. Lightwave Technol. **22**, 977 (2004).
8. J. P. Gordon and H. Kogelnik, Proc. Natl. Acad. Sci. U.S.A. **97**, 4541 (2000).
9. A. Galtarossa, L. Palmieri, M. Schiano, and T. Tambosso, Opt. Lett. **26**, 962 (2001).
10. C. W. Gardiner, *Handbook of Stochastic Methods*, 2nd ed. (Springer, New York, 1985).